Statistical Evaluation of UV/TiO_2/H_2O_2 and Fe^{2+}/H_2O_2 Process for the Treatment of Coloured Wastewater; A Comparative Study

I. Grčić, D. Vujević,* and N. Koprivanac
Faculty of Chemical Engineering and Technology, University of Zagreb, Marulićev Trg 19, HR-10000, Zagreb, Croatia

Original scientific paper
Received: November 17, 2009
Accepted: September 7, 2010

In this work, two types of advanced oxidation processes; photocatalytic oxidation, UV/TiO_2/H_2O_2 and classic Fenton oxidation, Fe^{2+}/H_2O_2, have been applied for the treatment of a model wastewater containing reactive azo dyes, C.I. Reactive Violet 2 (RV2) and C.I. Reactive Yellow 3 (RY3). In order to evaluate the effect of the initial concentration of catalysts, $\gamma(TiO_2)$ or $[Fe^{2+}]$, initial concentration of oxidant, $[H_2O_2]$ or the initial oxidant/catalyst mole ratio $[H_2O_2]/[Fe^{2+}]$ and pH on apparent mineralization and decolourization rates, a response surface method (RSM) D-optimal design was used. Mineralization was described by pseudo-first-order kinetics with the highest observed rate constants; $k_{m,UV} = 0.0065$ min^{-1} in the case of UV/TiO_2/H_2O_2 process and $k_{m,F} = 0.0213$ min^{-1} in the case of Fenton process. A kinetic model describing decolourization on wavelengths of maximum absorbance for studied dyes, λ_{maxRV2} 550 nm, and λ_{maxRY3} 385 nm, was composed of two first-order in-series reactions with corresponding decolourization rates. The effects of each factor on the efficiency of the applied processes were found to be significant.

Key words:
Wastewater treatment, reactive azo dyes, photocatalytic oxidation, Fenton oxidation, response surface method (RSM), D-optimal design

Introduction

The intensive growth of the human population and rapid industrial development consequently lead to the generation of a tremendous amount of waste, municipal and industrial wastewater, as well as environmental pollution in general. Coloured wastewaters originating from organic dye manufacturing and application industries present a significant environmental issue regarding intensive colouration which is visible even at very small amounts of dyes in water (μg dm^{-3}). These flows are also burdened with various organic compounds, intermediates and by-products unacceptable for the environment. Moreover, limited transparency of light has negative effects on the metabolism of aquatic flora and fauna.[1] A group of reactive dyes largely participates in the total amount of various dyes produced and applied worldwide annually. In general, the methods for coloured wastewater treatment can be classified as biological, physical and chemical methods.[2] Despite the certain advantages of biological methods, they are ineffective for degradation of reactive dyes due to their complex aromatic structure, stability and mostly non-biodegradability. Physical methods of coloured wastewater treatment (adsorption, flocculation/coagulation, membrane processes, ion exchange),[3] generally transfer the pollution from one phase to another, are often the most expensive and are ecologically inefficient. Engagement of secondary waste disposal and adsorbents regeneration additionally decreases the economic efficiency of these processes. An alternative to the conventional coloured wastewater treatment processes are advanced oxidation processes (AOPs), which can be applied individually or as part of an integral treatment process. The advantage of these processes in comparison with conventional wastewater treatment methods is the possibility of complete degradation of the organic load to water and carbon dioxide, due to reactions with nonselective and highly reactive free radicals, e.g. •OH.[4]

The response surface method (RSM) is a statistical mathematical technique used for modelling and optimization of the process in which a response of interest is influenced by several variables. The RSM has an important application in the design, development and formulation of new products, as well as in the improvement of existing product design. It defines the effect of the independent variables on the process either individually or collectively. Further, the experimental methodology generates a mathematical model, which describes the chemical or biochemical processes. The response surface method has been very popular for optimization studies in recent years. The design procedure of the RSM is as follows:[5]

*Corresponding author: Tel.: +385 1 4597 123; fax: +385 1 459 143; E-mail address: dvujev@fkit.hr

– Designing of experiments for adequate and reliable measurement of the response(s) of interest

– developing a predictive statistical model with the best fittings

– representing the direct and interactive effects of process parameters through two and/or three-dimensional plots.

The objective of this study was to treat the simulated dye wastewater containing C.I. Reactive Violet 2 (RV2) and C.I. Reactive Yellow 3 (RY3) by photocatalysis with TiO_2 and additional oxidant, hydrogen peroxide (UV/TiO_2/H_2O_2) as well as classical Fenton [Fe^{2+}]/[H_2O_2]. The role of hydrogen peroxide is considered different depending on the process. As eqs. (1) to (8) describe the reactions occurring within UV/TiO_2/H_2O_2 process, it can be seen that the addition of H_2O_2 results with a higher formation of •OH radicals due to (i) direct photolysis of H_2O_2 (eq. (2)), and (ii) electron scavenging (eq. (8)).

$$TiO_2 + h\nu \rightarrow TiO_2\ (e^- + h^+) \quad (1)$$

$$H_2O_2 + h\nu \rightarrow 2\ \bullet OH \quad (2)$$

$$TiO_2\ (h^+) + H_2O_{ad} \rightarrow TiO_2 + \bullet OH_{\ ad} + H^+ \quad (3)$$

$$TiO_2\ (h^+) + OH^-_{ad} \rightarrow TiO_2 + \bullet OH_{\ ad} \quad (4)$$

$$TiO_2\ (e^-) + O_2 \rightarrow TiO_2 + O_2^-\bullet \quad (5)$$

$$O_2^-\bullet + H_2O \rightarrow HO_2\bullet + OH^- \quad (6)$$

$$2\ HO_2\bullet \rightarrow O_2 + H_2O_2 \quad (7)$$

$$TiO_2\ (e^-) + H_2O_2 \rightarrow TiO_2 + OH^- + \bullet OH \quad (8)$$

Thus, H_2O_2 enhances the overall photodegradation rate.[6] On the other hand, H_2O_2 as an undivided part of Fenton reagent, represents the most used oxidant that makes Fenton oxidation possible, eq. (9).[2,7]

$$Fe^{2+} + H_2O_2 \rightarrow Fe^{3+} + HO^- + HO\bullet \quad (9)$$

To evaluate decolourization and mineralization extent achieved by applied processes, as a function of key operating parameters, a response surface method (RSM), particularly D-optimal design was used. Mineralization was monitored in terms of total organic carbon (TOC) measurements, and decolourization of the studied dyes was obtained by monitoring colour removal based on UV/VIS spectrophotometric measurements on a wavelength of maximal absorbance for the studied dyes, i.e. λ_{maxRV2} 550 nm, and λ_{maxRY3} 385 nm.

Materials and methods

All reagents in this work were analytical reagent grade and used with no further purification, supplied by Ciba-Geigy, Switzerland (reactive dyes, RY3 and RV2), Degussa, Germany (TiO_2, P25, mainly anatase) and Kemika, Zagreb (ferrous sulphate ($FeSO_4 \cdot 7H_2O$)), hydrogen peroxide (w = 30 %), potassium hydroxide and sulphuric acid). Experiments were performed using model dye wastewaters consisting of RV2 and RY3 mixture in concentration of γ = 50 mg dm^{-3} each. The initial pH of the studied system was varied using KOH or H_2SO_4 (c = 1 mol dm^{-3}), followed by the addition of ferrous sulphate in the case of Fenton process. All experiments were performed in a batch (photo) reactor of V = 0.8 dm^3 total volume. The radiation source was low pressure mercury UV lamp (8W, UV-C 254 nm, UVP-Ultra Violet Products, Cambridge, UK) which was placed axial in a quartz tube inside the reactor, in case of experiments that involve photocatalytic oxidation, UV/TiO_2/H_2O_2. The reactor was made of borosilicate glass, with sampling ports on the top, magnetic stirrer and water jacket for temperature control.[8] The reaction temperature was kept at 20 ± 2 °C. Samples were collected in certain periods of time within 120 min. Samples were analyzed directly after filtration (Chromafil RC 45/25, Macherey-Nagel, Germany). In the case of Fenton

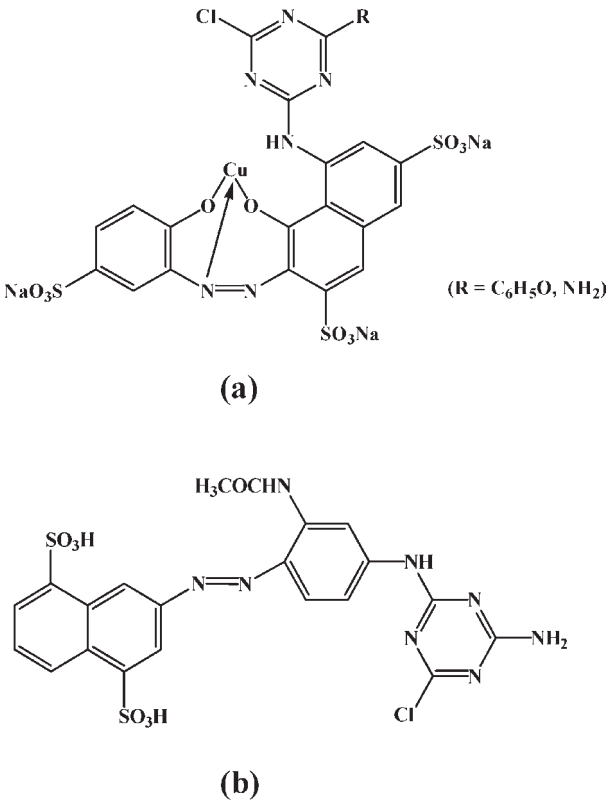

Fig. 1 – *Structure of the studied reactive dyes, RV2 (a) and RY3 (b)*

process, a grain or two of KOH was added to each sample in order to precipitate iron hydroxides and remove possible absorption interference below λ = 400 nm, and were then subjected to further analyses.

The mineralization extent was determined on the basis of total organic carbon (TOC) content measurements, performed by using TOC analyzer; TOC-V_{CPN} 5000 A, Shimadzu. A Perkin Elmer Lambda EZ 201 UV/VIS spectrophotometer was used for monitoring decolourization at two different wavelengths, i.e. λ = 385 nm and 550 nm that correspond to absorption maxima of RY3 and RV2. The concentration of each dye was determined on the basis of UV/VIS absorption at λ_{max}, by applying the Lambert-Beer equation to the measured absorbances at their respective λ_{max}. The pH values were measured by Handylab pH/LF portable pH/conductivity meter, Schott Instruments GmbH, Mainz, Germany.

Experimental design and statistical analysis

A three-factor RSM D-optimal design was used to examine the influence of the operating conditions on mineralization and decolourization rates. Based on previous experience on applied processes and according to the data presented in related works,[8–11] (X_{1UV}) initial TiO_2 mass concentration, (X_{2UV}) initial hydrogen peroxide concentration and (X_{3UV}) initial pH, were chosen as the determining factors for the performance of photocatalytic oxidation, i.e. UV/TiO_2/H_2O_2 process; while (X_{1F}) initial Fe^{2+} concentration, (X_{2F}) oxidant/catalyst mole ratio i.e. [H_2O_2]/[Fe^{2+}] and (X_{3F}) initial pH, were chosen as the key operating factors for the Fenton process (Table 1). These parameters (X_1, X_2, X_3) have been identified as control factors (CFs) because the variation of their values resulted in optimal performance. Other parameters, i.e., temperature and stirring speed were set at fixed values. The method consisted of (i) defining levels, (ii) selection of the model that fits, and (iii) choosing design points, *h*, from the set of *n* candidate points generated depending on the selected model. As presented in Table 1, each CF is varied over 3 levels. D-optimal design as a technique demands selection of the model at the beginning. That could be difficult if there were no expectations of what the model should be. In this particular case, there is some allusion about the model.[9,11,12] In the frame of this work, a two-factor-interaction model (2FI) was used for statistical evaluation of applied processes for the treatment of coloured wastewater, eq. (10)

Table 1 – *Actual factors and their levels*

CFs		Levels		
		1 (low)	2	3 (high)
UV/TiO_2/H_2O_2 process				
X_{1UV}	γ(TiO_2)/mg dm^{-3}	100	550	1000
X_{2UV}	[H_2O_2]/mmol dm^{-3}	0.5	5.25	10
X_{3UV}	pH	3	5.5	8
[Fe^{2+}]/[H_2O_2] process				
X_{1F}	[Fe^{2+}]/mmol dm^{-3}	0.25	1.13	2
X_{2F}	[H_2O_2]/[Fe^{2+}]	2	26	50
X_{3F}	pH	2	2.75	3.5

$$Y = b_{0i} + b_{1i}X_{1i} + b_{2i}X_{2i} + b_{3i}X_{3i} + \\ + b_{12i}X_{1i}X_{2i} + b_{13i}X_{1i}X_{3i} + b_{23i}X_{2i}X_{3i} \quad (10)$$

where b_n is the coefficient associated with each n^{th} factor, and the letters, X_1, X_2, X_3, represent the factors in the model. Index *i* refers to the studied process. For photocatalytic oxidation *i* becomes "$_{UV}$", while in the case of Fenton process, *i* becomes "$_F$". Combination of factors (such as $X_{1i}X_{2i}$) represents interactions between the individual factors.

Regarding the selected model, for the given combination of the k factors, a set of n candidate points (29) were generated. The objective of D-optimal design was to select h design points from that set by embedded algorithm, which resulted in 7 minimum model points, k+1 (4) points for estimation of lack-of-fit and replicates as well. Finally, an experimental plan with 15 experiments was made for each applied process (Tables 2 and 3). Tables 2 and 3 also show the standard array for three CFs and 15 experiments, run order and the observed responses. The experiments were performed in a random manner in order to avoid any systematic bias in the outcomes.

The obtained statistical models were evaluated for each response function and the experimental data (the apparent mineralization and decolourization rate coefficients) were analyzed statistically applying analysis of variance (ANOVA) and using *Design-Expert 6.0.6,* a DoE software tool from Stat-Ease, Inc. The adequacy of the final models was verified by graphical and numerical analysis.

Table 2 – *Experimental plan and results for UV/TiO_2/H_2O_2 process*

Run	CFs level			Responses				
	X_{1UV}	X_{2UV}	X_{3UV}	Y_{1UV} k_{mUV}/min^{-1}	Y_{2UV} $k_{1,550\ UV}$/min^{-1}	Y_{3UV} $k_{2,550\ UV}$/min^{-1}	Y_{4UV} $k_{1,385\ UV}$/min^{-1}	Y_{5UV} $k_{2,385\ UV}$/min^{-1}
1	3	1	3	0.0037	0.014	0.007	0.011	0.0031
2	1	3	3	0.0034	0.036	0.017	0.020	0.0082
3	3	1	3	0.0039	0.014	0.009	0.010	0.0029
4	1	3	1	0.0039	0.027	0.011	0.018	0.0074
5	1	1	1	0.0011	0.008	0.002	0.008	0.0022
6	2	1	1	0.0041	0.017	0.007	0.010	0.0045
7	1	3	3	0.0033	0.034	0.015	0.020	0.0106
8	1	1	3	0.0009	0.007	0.002	0.009	0.0015
9	2	2	2	0.0045	0.031	0.015	0.021	0.0082
10	3	3	3	0.0025	0.022	0.013	0.018	0.0091
11	3	1	1	0.0035	0.019	0.014	0.011	0.0053
12	3	3	3	0.0025	0.020	0.014	0.018	0.0107
13	1	1	3	0.0010	0.008	0.003	0.009	0.0011
14	1	2	1	0.0032	0.020	0.006	0.015	0.0038
15	3	3	1	0.0065	0.040	0.013	0.031	0.0090

Table 3 – *Experimental plan and results for Fe^{2+}/H_2O_2 process*

Run	CFs level			Responses				
	X_{1F}	X_{2F}	X_{3F}	Y_{1F} k_{mF}/min^{-1}	Y_{2F} $k_{1,550\ F}$/min^{-1}	Y_{3F} $k_{2,550\ F}$/min^{-1}	Y_{4F} $k_{1,385\ F}$/min^{-1}	Y_{5F} $k_{2,385\ F}$/min^{-1}
1	1	3	1	0.0081	0.617	0.029	0.574	0.009
2	3	3	1	0.0213	0.739	0.115	0.679	0.099
3	2	1	1	0.0080	0.947	0.008	0.894	0.007
4	2	2	2	0.0137	0.839	0.058	0.716	0.051
5	3	1	1	0.0152	0.896	0.017	0.825	0.009
6	1	3	3	0.0099	0.455	0.062	0.339	0.050
7	1	3	1	0.0098	0.423	0.060	0.396	0.049
8	1	3	3	0.0098	0.450	0.061	0.396	0.054
9	3	3	1	0.0210	0.739	0.115	0.698	0.092
10	1	1	3	0.0081	0.671	0.030	0.583	0.021
11	3	3	3	0.0211	0.739	0.115	0.702	0.099
12	1	1	3	0.0080	0.606	0.025	0.576	0.023
13	3	1	3	0.0151	0.955	0.019	0.904	0.014
14	3	3	3	0.0208	0.739	0.116	0.672	0.095
15	1	2	1	0.0090	0.563	0.046	0.447	0.032

Results and discussion

Kinetic studies

In both the applied processes, UV/TiO_2/H_2O_2 and Fe^{2+}/H_2O_2, the residual content of total organic carbon was monitored over 60 min and a mineralization rate was modelled using eq. (11)

$$-\mathrm{d}\gamma_{TOC}/\mathrm{d}t = k_{mi}\,\gamma_{TOC} \Rightarrow \gamma_{TOC}/\gamma_{TOC,0} = \mathrm{e}^{-k_m t} \quad (11)$$

where i = {UV, F}

regarding the general mass balance for a well-mixed, constant volume and constant temperature batch reactor, with the following boundary conditions; $t = 0$, $\gamma_{TOC} = \gamma_{TOC,0}$. In eq. (11), k_{mi} is the reaction rate constant, referred to hereinafter as apparent mineralization rate constant (min^{-1}), γ_{TOC} is the TOC content (mg dm^{-3}), and ($-d\gamma_{TOC}/dt$) is the first order mineralization (TOC removal) rate. In order to determine the apparent mineralization rate constant, $-\ln(\gamma_{TOC}/\gamma_{TOC,0})$ was plotted against reaction time (Fig. 2).

Furthermore, decolourization kinetics and respective rates obtained within the applied processes were investigated. According to the literature,[13–15] a simple first-order model was unsuitable for describing the entire period of oxidation. As presented by eqs. (12) and (13), a two first-order in-series reaction model was introduced, describing a degradation of RV2 or RY3 to intermediates in the first step, and a consequent degradation of intermediates towards product with zero absorptivities at λ_{max} in the second step.

$$\mathrm{RV2} \xrightarrow{k_{1,550}} \underset{\text{(with zero absorptivities at 550 nm)}}{\text{intermediates}} \xrightarrow{k_{2,550}} \text{products} \quad (12)$$

$$\mathrm{RY3} \xrightarrow{k_{1,385}} \underset{\text{(with zero absorptivities at 385 nm)}}{\text{intermediates}} \xrightarrow{k_{2,385}} \text{products} \quad (13)$$

Assuming that both reactions followed first-order kinetics, the batch model for the concentration of the studied dyes, c_{RV2} and c_{RY3}, and the intermediates, $c_{CI,550}$ and $c_{CI,385}$, with time could be described by eqs. (14) and (15), with the following boundary conditions; $t = 0$, $c_{RV2} = c_{RV2,0}$, $c_{RY3} = c_{RY3,0}$, $c_{CI,550} = 0$, $c_{CI,385} = 0$.

$$-\mathrm{d}c_{RV2}/\mathrm{d}t = k_{1,550}\,c_{RV2} \Rightarrow c_{RV2}/c_{RV2,0} = \mathrm{e}^{-k_{1,550}t} \quad (14a)$$

$$-\mathrm{d}c_{RY3}/\mathrm{d}t = k_{1,385}\,c_{RY3} \Rightarrow c_{RY3}/c_{RY3,0} = \mathrm{e}^{-k_{1,385}t} \quad (14b)$$

$$\mathrm{d}c_{CI,550}/\mathrm{d}t = k_{1,550}\,c_{RV2} - k_{2,550}\,c_{CI,550} \Rightarrow$$
$$\Rightarrow c_{CI,550} = [k_{1,550}\,c_{RV2,0}/(k_{2,550} - k_{1,550})] \cdot \quad (15a)$$
$$\cdot (\mathrm{e}^{-k_{1,550}t} - \mathrm{e}^{-k_{2,550}t})$$

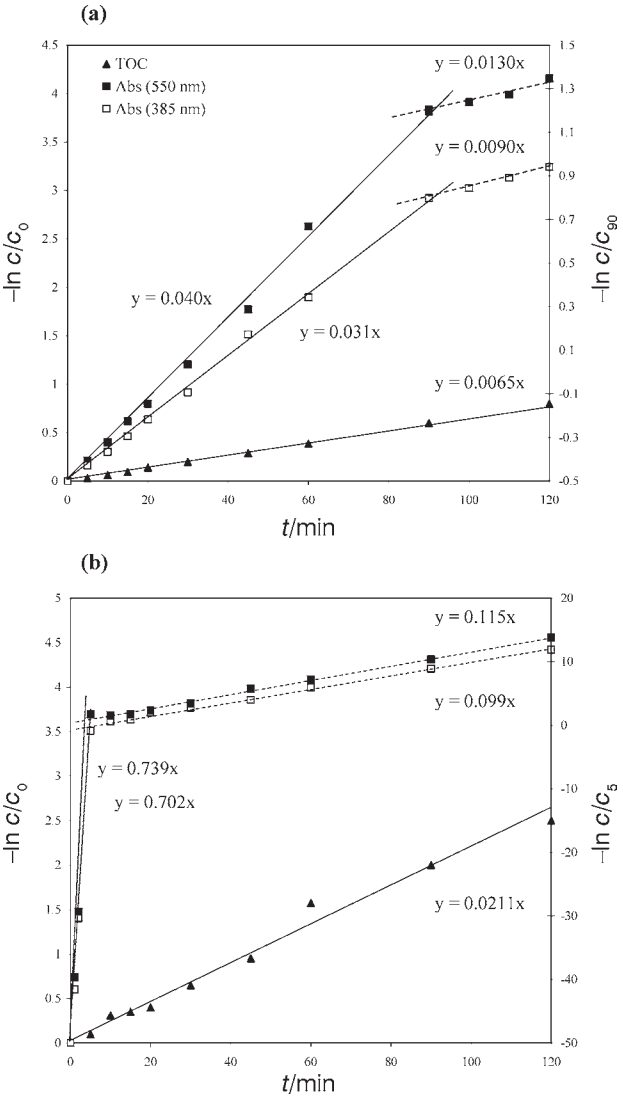

Fig. 2 – *Example of mineralization and decolourization kinetics for photocatalytic oxidation, Run 15 (a) and Fenton process, Run 11 (b)*

$$\mathrm{d}c_{CI,385}/\mathrm{d}t = k_{1,385}\,c_{RY3} - k_{2,385}\,c_{CI,385} \Rightarrow$$
$$\Rightarrow c_{CI,385} = [k_{1,385}\,c_{RY3,0}\,/\,(k_{2,385} - k_{1,385})] \cdot \quad (15b)$$
$$\cdot (\mathrm{e}^{-k_{1,385}t} - \mathrm{e}^{-k_{2,385}t})$$

The measured absorbances are the sum of contributions from the dyes and intermediates. With this in mind, eqs. (14) and (15) could be combined with Lambert-Beer's law giving the following eq. (16).

$$\mathrm{abs}_{550,t}/\mathrm{abs}_{550,0} = \mathrm{e}^{-k_{1,550}t} + \left(\varepsilon_{CI,550}/\varepsilon_{RV2}\right) \cdot$$
$$\cdot \left[k_{1,550}/(k_{2,550} - k_{1,550})\right] \cdot (\mathrm{e}^{-k_{1,550}t} - \mathrm{e}^{-k_{2,550}t}) \quad (16a)$$

$$\mathrm{abs}_{385,t}/\mathrm{abs}_{385,0} = \mathrm{e}^{-k_{1,385}t} + \left(\varepsilon_{\mathrm{CI},385}/\varepsilon_{\mathrm{RY3}}\right)\cdot \cdot\left[k_{1,385}/(k_{2,385} - k_{1,385})\right]\cdot(\mathrm{e}^{-k_{1,385}t} - \mathrm{e}^{-k_{2,385}t}) \quad (16b)$$

where ε_{RV2}, ε_{RY3} and $\varepsilon_{CI,550}$, $\varepsilon_{CI,385}$ represent molar extinction coefficients of RV2, RY3 and their intermediates, respectively.

Furthermore, some simplifications of the first-order in-series reaction model were made for each process. Regarding the knowledge of Fenton oxidation's, $[Fe^{2+}]/[H_2O_2]$, high efficiency due to the fast and constant generation of hydroxyl radicals, it could be assumed that after 5 min, the concentration of the studied dyes, RV2 and RY3, became negligible compared to intermediates concentration, leading to the fact that the measured absorbance in the fifth minute of the process depended only on the concentration of intermediates. Moreover, oxidation occurring after the fifth minute could be considered as a stand-alone process of intermediates degradation. In the first 5 min, the concentration of the dyes is eligible and due to the high molar extinction coefficient of each dye at its λ_{max}, it could be stated that absorbance is contributed solely by studied dyes. These statements were described as follows, eqs. (17) and (18);

$$\mathrm{abs}_{t_{t\to5}}/\mathrm{abs}_0 = \mathrm{e}^{-k_{1F}t} \quad (17)$$

$$\mathrm{abs}_{5\ \mathrm{min}} \equiv \mathrm{abs'}_0 \Rightarrow \mathrm{abs}_{t_{5\to120}}/\mathrm{abs'}_0 = \mathrm{e}^{-k_{2F}t} \quad (18)$$

Finally, $-\ln(\mathrm{abs}_t/\mathrm{abs}^{(')}_0)$ were plotted against the reaction time to determine the decolourization rate constants (Fig. 2b).

In comparison with Fenton oxidation, the decolourization rate constants achieved by photocatalytic oxidation, UV/TiO_2/H_2O_2, were somewhat slower. Therefore, in order to neglect concentration of the studied dyes, RV2 and RY3, a period of 90 min is necessary (Fig. 2a). In this case, within the first 90 min, the concentration of the dyes is eligible and due to the high molar extinction coefficient of each dye at its λ_{max}, absorbances are contributed solely by studied dyes, as described by eqs. (19) and (20);

$$\mathrm{abs}_{t_{t\to90}}/\mathrm{abs}_0 = \mathrm{e}^{-k_{1UV}t} \quad (19)$$

$$\mathrm{abs}_{90\mathrm{min}} \equiv \mathrm{abs'}_0 \Rightarrow \mathrm{abs}_{t_{90\to120}}/\mathrm{abs'}_0 = \mathrm{e}^{-k_{2UV}t} \quad (20)$$

Assuming that each reaction followed first-order kinetics, $-\ln(\mathrm{abs}_t/\mathrm{abs}^{(')}_0)$ was plotted against reaction time, and decolourization rate constants were determined (Fig. 2a).

Considering photocatalytic oxidation, i.e. UV/TiO_2/H_2O_2 process, the photodegradation and adsorption of model pollutants can be well described by the Langmuir-Hinshelwood (L-H) kinetic model.[16] If the reactant is more strongly adsorbed on the surface than the products, and when both the reactant and solvent are adsorbed on the surface without competing for the same active sites, then the rate of a unimolecular surface reaction, r, is proportional to surface coverage, Θ and will follow eq. (21),

$$r = -\frac{\mathrm{d}c}{\mathrm{d}t} = k_\mathrm{r}\Theta = \frac{k_\mathrm{r}Kc_0}{1 + Kc_0} \quad (21)$$

where k_r = reaction rate constantt, Θ = fraction of the surface covered by the reactant, K = adsorption coefficient of the reactant, c_0 = initial concentration of the reactant. Integration of eq. (21) yields with eq. (22),

$$-\ln\frac{c_\mathrm{t}}{c_0} + K(c_0 - c_t) = k_\mathrm{r}Kt \quad (22)$$

However, when c_0 is very small and a reactant is strongly adsorbed, eq. (22) reduces to eq. (23);

$$-\ln\frac{c_\mathrm{t}}{c_0} = k_\mathrm{app}t \quad (23)$$

where k_{app} represents the apparent first order rate coefficient.[16,17] Therefore, mineralization and decolourization rate constants presented in this work were well determined by plotting $\ln(\gamma_{TOC}/\gamma_{TOC,0})$ and $-\ln(\mathrm{abs}_t/\mathrm{abs}^{(')}_0)$ vs. reaction time.

Interpretation of statistical analyses

The statistical study of the processes, UV/TiO_2/H_2O_2 and $[Fe^{2+}]/[H_2O_2]$, was performed using response surface methodology (RSM), particularly by a D-optimal design. Individual parameters and their interaction effects on the apparent mineralization and decolourization rate coefficients were determined and statistical process models were developed, according to the modified two-factor interaction (2FI) or quadratic model. The predictive models are described in eq. (10) (2FI), and eq. (24) (quadratic).

$$Y = b_{0i} + b_{1i}X_{1i} + b_{2i}X_{2i} + b_{3i}X_{3i} + b_{11i}X_{1i}^2 + b_{22i}X_{2i}^2 + b_{33i}X_{3i}^2 + b_{12i}X_{1i}X_{2i} + b_{13i}X_{1i}X_{3i} + b_{23i}X_{2i}X_{3i} \quad (24)$$

Multiple regression analysis of the experimental data using *Design-Expert* software resulted in model equations describing the dependency of responses (Y_{1UV}, Y_{2UV}, Y_{3UV}, Y_{1F}, Y_{2F}, Y_{3F}) to the selected process parameters and interactions.

Since special emphasis was put on the kinetics, so the final response surface predictive models given in actual terms regarding responses Y_{1i} (actual; k_{mi}/min^{-1}), Y_{2i} (actual $k_{1,550\ i}/\mathrm{min}^{-1}$), Y_{3i} (actual $k_{2,550\ i}/\mathrm{min}^{-1}$), Y_{4i} (actual $k_{1,385\ i}/\mathrm{min}^{-1}$) and Y_{5i} (actual $k_{2,385\ i}/\mathrm{min}^{-1}$) are stated below, eqs. (25) and (26).

$$k_{m\ UV}/\text{min}^{-1} = 1.35 \cdot 10^{-3} + 3.17 \cdot 10^{-6}\ \gamma(TiO_2) + \\ + 5.12 \cdot 10^{-4}\ [H_2O_2] - 8.53 \cdot 10^{-5}\ \text{pH} - \\ - 2.81 \cdot 10^{-7}\ \gamma(TiO_2)[H_2O_2] - 3.75 \cdot 10^{-5}\ [H_2O_2]\ \text{pH} \quad (25a)$$

$$k_{1,550\ UV}/\text{min}^{-1} = 9.85 \cdot 10^{-4} + 3.11 \cdot 10^{-5}\ \gamma(TiO_2) + \\ + 2.73 \cdot 10^{-3}\ [H_2O_2] + 8.56 \cdot 10^{-4}\ \text{pH} - \\ - 1.52 \cdot 10^{-6}\ \gamma(TiO_2)[H_2O_2] - 3.41 \cdot 10^{-6}\ \gamma(TiO_2)\ \text{pH} \quad (25b)$$

$$k_{2,550\ UV}/\text{min}^{-1} = 5.08 \cdot 10^{-3} + 8.77 \cdot 10^{-6}\ \gamma(TiO_2) + \\ + 2.10 \cdot 10^{-3}\ [H_2O_2] - 6.06 \cdot 10^{-4}\ \text{pH} - \\ - 1.01 \cdot 10^{-6}\ \gamma(TiO_2)[H_2O_2] \quad (25c)$$

$$k_{1,385\ UV}/\text{min}^{-1} = 1.89 \cdot 10^{-3} + 1.35 \cdot 10^{-5}\ \gamma(TiO_2) + \\ + 1.96 \cdot 10^{-3}\ [H_2O_2] + 9.73 \cdot 10^{-4}\ \text{pH} - \\ - 1.72 \cdot 10^{-6}\ \gamma(TiO_2)\ \text{pH} - 1.23 \cdot 10^{-4}\ [H_2O_2]\ \text{pH} \quad (25d)$$

$$k_{2,385\ UV}/\text{min}^{-1} = 3.33 \cdot 10^{-3} + 1.94 \cdot 10^{-6}\ \gamma(TiO_2) + \\ + 2.81 \cdot 10^{-4}\ [H_2O_2] - 3.14 \cdot 10^{-4}\ \text{pH} - \\ - 5.86 \cdot 10^{-5}\ [H_2O_2]\ \text{pH} \quad (25e)$$

$$k_{m\ F}/\text{min}^{-1} = - 0.0373 - 6.65 \cdot 10^{-3}\ [Fe^{2+}] + \\ + 2.49 \cdot 10^{-5}\ ([H_2O_2]/[Fe^{2+}]) + 0.0367\ \text{pH} + \\ + 4.71 \cdot 10^{-3}\ [Fe^{2+}]^2 - 6.68 \cdot 10^{-3}\ \text{pH}^2 + \\ + 4.48 \cdot 10^{-5}\ [Fe^{2+}]\ ([H_2O_2]/[Fe^{2+}]) \quad (26a)$$

$$k_{1,550\ F}/\text{min}^{-1} = 0.469 + 0.646\ [Fe^{2+}] - \\ - 3.95 \cdot 10^{-3}\ ([H_2O_2]/[Fe^{2+}]) + \\ + 9.11 \cdot 10^{-3}\ \text{pH} - 0.213\ [Fe^{2+}]^2 \quad (26b)$$

$$k_{2,550\ F}/\text{min}^{-1} = 0.0226 - 7.48 \cdot 10^{-3}\ [Fe^{2+}] + \\ + 5.35 \cdot 10^{-4}\ ([H_2O_2]/[Fe^{2+}]) + \\ + 1.49 \cdot 10^{-3}\ \text{pH} + 7.68 \cdot 10^{-4}\ [Fe^{2+}]\ ([H_2O_2]/[Fe^{2+}]) \quad (26c)$$

$$k_{1,385\ F}/\text{min}^{-1} = 1.65 + 0.758\ [Fe^{2+}] - \\ - 1.82 \cdot 10^{-3}\ ([H_2O_2]/[Fe^{2+}]) - 1.02\ \text{pH} - \\ - 0.260\ [Fe^{2+}]^2 + 0.191\ \text{pH}^2 - \\ - 7.38 \cdot 10^{-4}\ ([H_2O_2]/[Fe^{2+}])\ \text{pH} \quad (26d)$$

$$k_{2,385\ F}\ \text{min}^{-1} = - 3.39 \cdot 10^{-3} - 3.75 \cdot 10^{-3}\ [Fe^{2+}] + \\ + 9.21 \cdot 10^{-4}\ ([H_2O_2]/[Fe^{2+}]) + 6.98 \cdot 10^{-3}\ \text{pH} + \\ + 5.88 \cdot 10^{-4}\ [Fe^{2+}]\ ([H_2O_2]/[Fe^{2+}]) - \\ - 1.20 \cdot 10^{-4}\ ([H_2O_2]/[Fe^{2+}])\ \text{pH} \quad (26e)$$

For the current study, each response surface model was evaluated using ANOVA (Table 4). Regarding the UV/TiO_2/H_2O_2 process, F-values ranging from 6.59 to 30.67 and p-values < 0.0500 imply that each model equation is significant. Predictive statistical models describing mineralization and decolourization rates achieved by [Fe^{2+}]/[H_2O_2] process involved some quadratic terms, X_1^2, X_3^2, resulting with enhanced significance. Namely, F-values are in the range from 126.15 to 5316.28 and the corresponding p-values are below 0.0001.

The examination of residuals was used to investigate the models adequacy. Fig. 3 a-e presents a normal probability plot of residuals for each response within each process, Y_{1UV}, Y_{1F}, Y_{2UV}, Y_{2F}, Y_{3UV}, Y_{3F}, Y_{4UV}, Y_{4F}, Y_{5UV}, Y_{5F}. In each case, there is no severe indication of non-normality and no evidence pointing to possible outliers. The normal plots presented in Fig. 3a-e are normally distributed and resemble a straight line. Also, residuals are structureless and contain no obvious patterns, so it can be concluded that the models are adequate. Furthermore, residuals vs. predicted plots are normally distributed and the equality of variance does not seem to be violated, as presented in Fig. 4a-e. The obtained r^2 values suggest the fit is good and a variation in the observed values can be explained by the chosen model (Table 4). The result of the analysis shown in Fig. 5a-e is in accordance with given r^2 values. Namely, predicted *vs.* actual plot that shows equality of experimental data (actual) with the one obtained by the model (predicted) for the same initial values follows the line $x = y$. In an ideal case when r^2 value would be 1, all points on the predicted vs. actual graph would lie on the line $x = y$.[11,18] The results obtained within this study prove model adequacy and it can be concluded that the given models describe the investigated system very well throughout the experimental range. Finally, graphical interpretations of these models are presented in Figs. 6 and 7. Fig. 6a-c shows a dependency of mineralization and decolourization rates achieved by UV/TiO_2/H_2O_2 process on CFs; mass concentration of photocatalyst, X_{1UV}, concentration of oxidant, X_{2UV} at fixed pH value (pH 3). As it can be seen, rate constants attain higher values as concentration of both TiO_2 and H_2O_2 increases, confirming a significant influence of both parameters on process efficiency. Also, when a concentration of these CFs is close to low level, the mineralization rate rapidly decreases (Fig. 6a). Combination of the effects of each CF, as well as the influence of third CF, initial pH value of the system on UV/TiO_2/H_2O_2 process efficiency in terms of mineralization, is presented in Fig. 8. It can be observed that neutral to acidic pH conditions favor mineralization of organic contaminants. Regarding [Fe^{2+}]/[H_2O_2] process, a depend-

Table 4 – *ANOVA results and fit summary*

Source	SS	DF	F-value	p-value	r^2	Model	Significant terms
Y_{1UV}							
total	$3.03 \cdot 10^{-5}$	14					
model	$2.73 \cdot 10^{-5}$	5	9.18	0.0045	0.9017	modified 2FI	X_1, X_2, X_3, X_1X_2, X_2X_3
residual error – lack of fit	$2.95 \cdot 10^{-6}$	3	2.89	0.1310			
Y_{2UV}							
total	$1.54 \cdot 10^{-3}$	14					
model	$1.36 \cdot 10^{-3}$	5	14.29	0.0005	0.8882	modified 2FI	X_1, X_2, X_3, X_1X_2, X_1X_3
residual error – lack of fit	$1.67 \cdot 10^{-4}$	4	3.39	0.0885			
Y_{3UV}							
total	$1.32 \cdot 10^{-3}$	14					
model	$9.55 \cdot 10^{-4}$	4	6.59	0.0073	0.8588	modified 2FI	X_1, X_2, X_3, X_1X_2
residual error – lack of fit	$4.50 \cdot 10^{-5}$	4	3.72	0.0711			
Y_{4UV}							
total	$5.62 \cdot 10^{-4}$	14					
model	$5.11 \cdot 10^{-4}$	5	17.75	0.0002	0.9079	modified 2FI	X_1, X_2, X_3, X_1X_3, X_2X_3
residual error – lack of fit	$3.54 \cdot 10^{-5}$	4	2.11	0.2267			
Y_{5UV}							
total	$1.45 \cdot 10^{-4}$	14					
model	$1.34 \cdot 10^{-4}$	4	30.67	<0.0001	0.9246	modified 2FI	X_1, X_2, X_3, X_2X_3
residual error – lack of fit	$8.32 \cdot 10^{-6}$	6	2.04	0.2446			
Y_{1F}							
total	$4.12 \cdot 10^{-4}$	14					
model	$4.12 \cdot 10^{-4}$	6	5316.28	<0.0001	0.9997	modified quadratic	X_1, X_2, X_3, X_1^2, X_3^2, X_1X_2
residual error – lack of fit	$3.47 \cdot 10^{-8}$	4	0.51	0.7377			
Y_{2F}							
total	0.42	14					
model	0.42	4	216.52	<0.0001	0.9886	modified quadratic	X_1, X_2, X_3, X_1^2
residual error – lack of fit	$2.72 \cdot 10^{-3}$	6	0.86	0.5875			
Y_{3F}							
total	0.022	14					
model	0.021	4	252.44	<0.0001	0.9902	modified 2FI	X_1, X_2, X_3, X_1X_2
residual error – lack of fit	$2.01 \cdot 10^{-4}$	6	0.92	0.5144			
Y_{4F}							
total	0.44	14					
model	0.43	6	126.15	<0.0001	0.9895	modified quadratic	X_1, X_2, X_3, X_1^2, X_3^2, X_2X_3
residual error – lack of fit	$2.36 \cdot 10^{-3}$	4	1.05	0.4809			
Y_{5F}							
total	0.017	14					
model	0.017	5	262.89	<0.0001	0.9932	modified 2FI	X_1, X_2, X_3, X_1X_2, X_2X_3
residual error – lack of fit	$7.34 \cdot 10^{-5}$	5	1.42	0.3779			

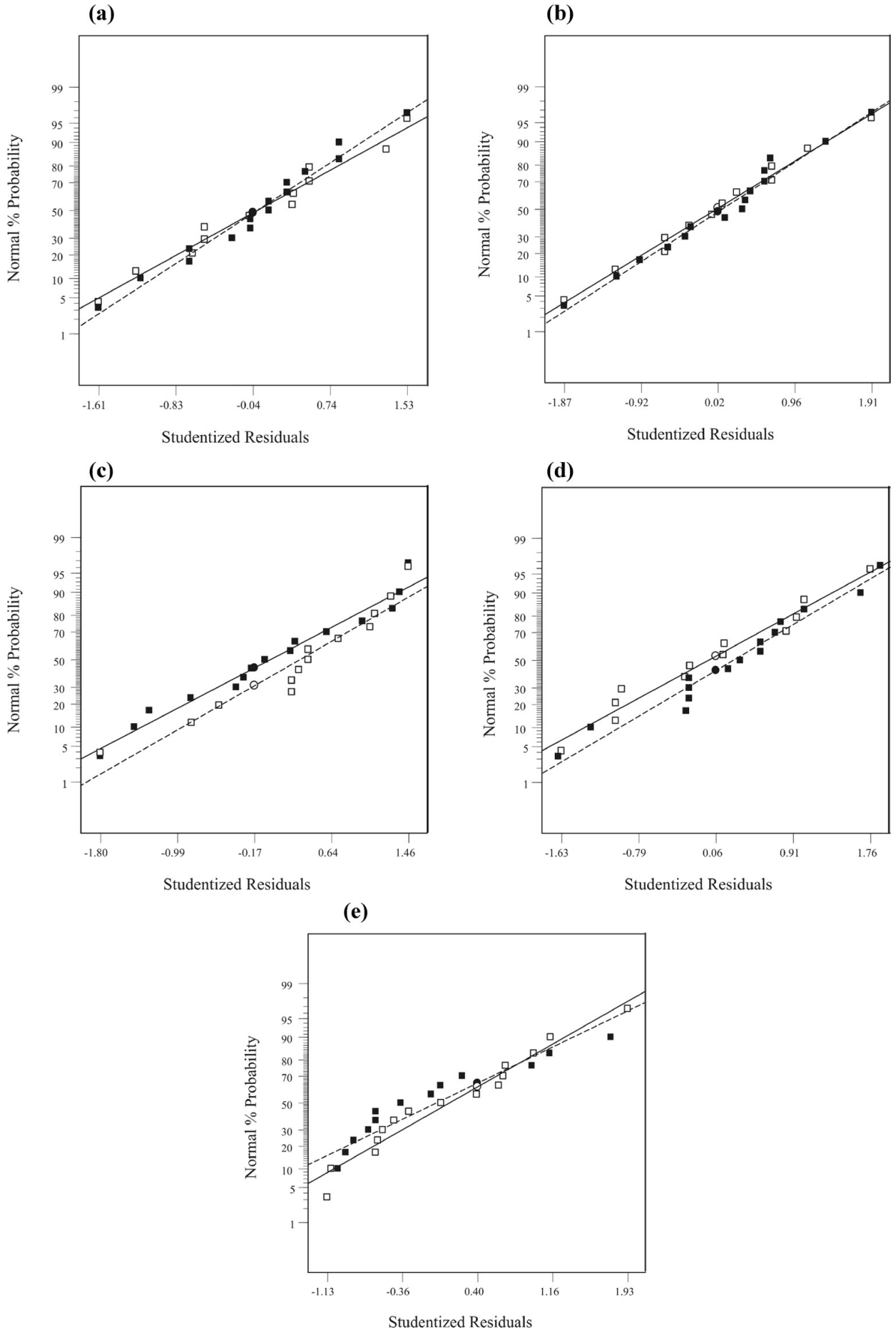

F i g . 3 – *Normal probability plot of residuals for each response; (a) k_m, (b) $k_{1,550}$, (c) $k_{2,550}$, (d) $k_{1,385}$, (e) $k_{2,385}$; regarding (--■--) UV/TiO_2/H_2O_2 and (--□--) [Fe^{2+}]/[H_2O_2] process*

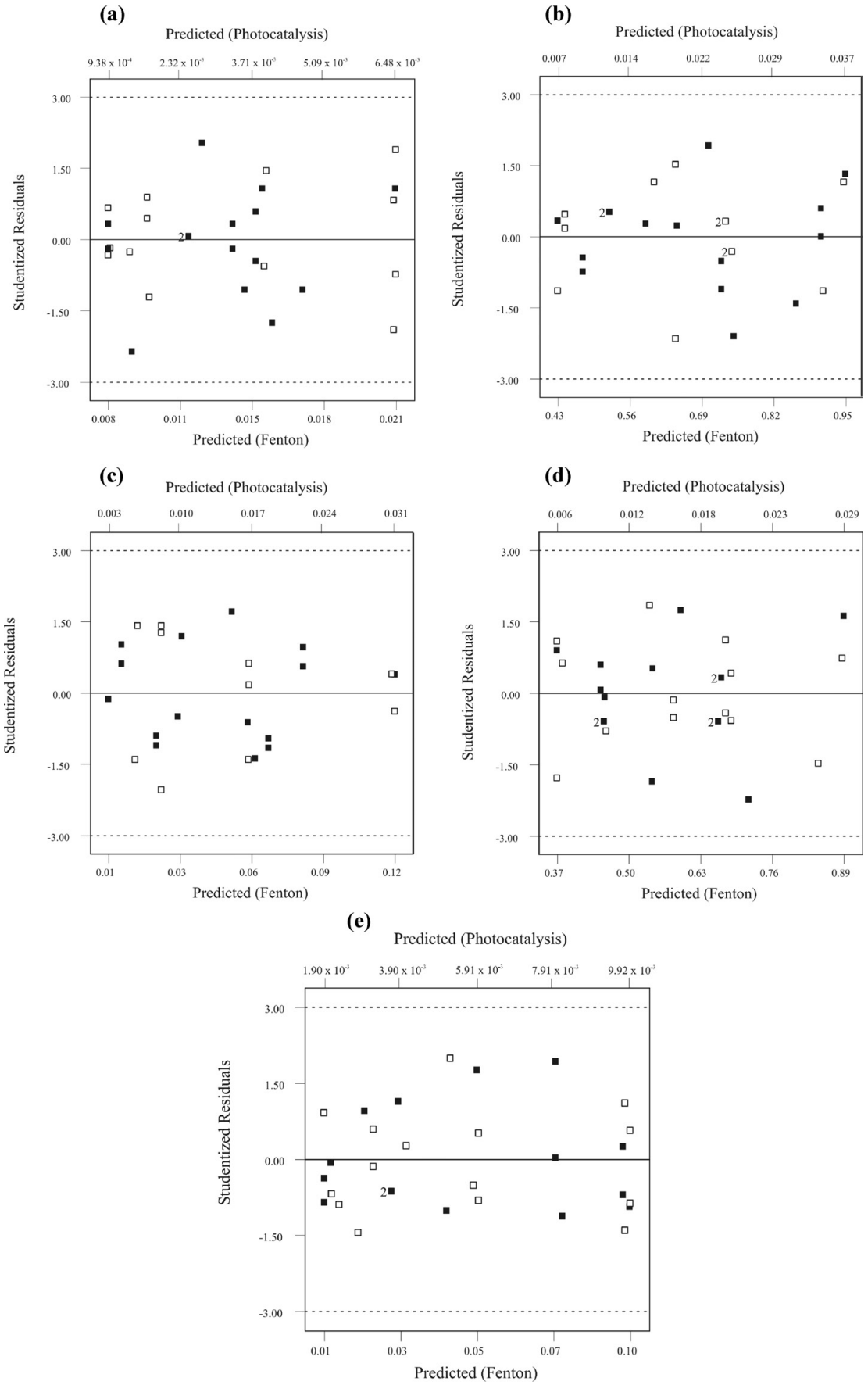

F i g . 4 – *Residuals vs. predicted plot for each response; (a) k_m, (b) $k_{1,550}$, (c) $k_{2,550}$, (d) $k_{1,385}$, (e) $k_{2,385}$; regarding (■) UV/TiO_2/H_2O_2 and (□) [Fe^{2+}]/[H_2O_2] process*

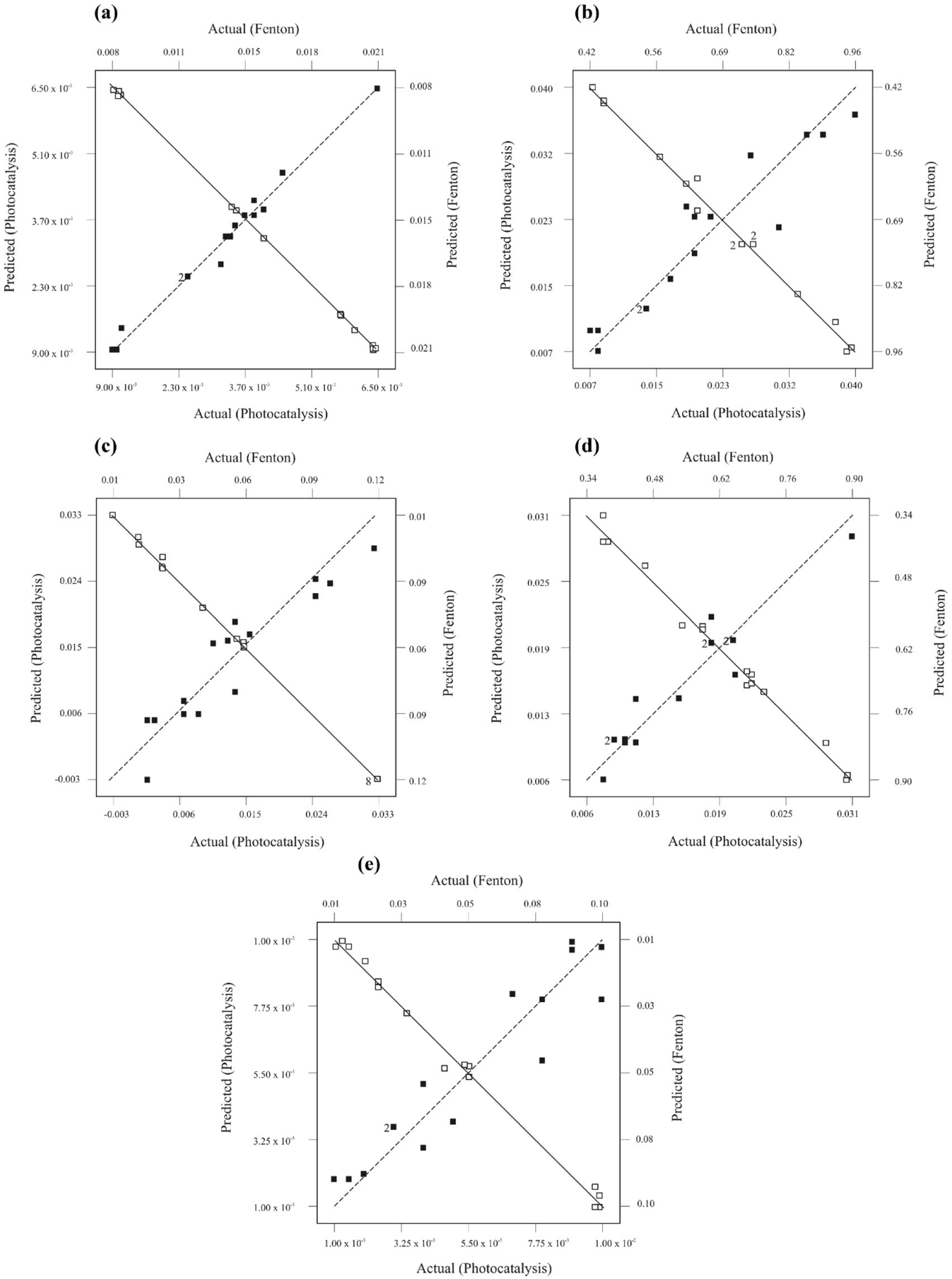

F i g . 5 – *Predicted vs. actual plot for each response; (a) k_m, (b) $k_{1,550}$, (c) $k_{2,550}$, (d) $k_{1,385}$, (e) $k_{2,385}$; regarding (--■--) UV/TiO_2/H_2O_2 and (--□--) [Fe^{2+}]/[H_2O_2] process*

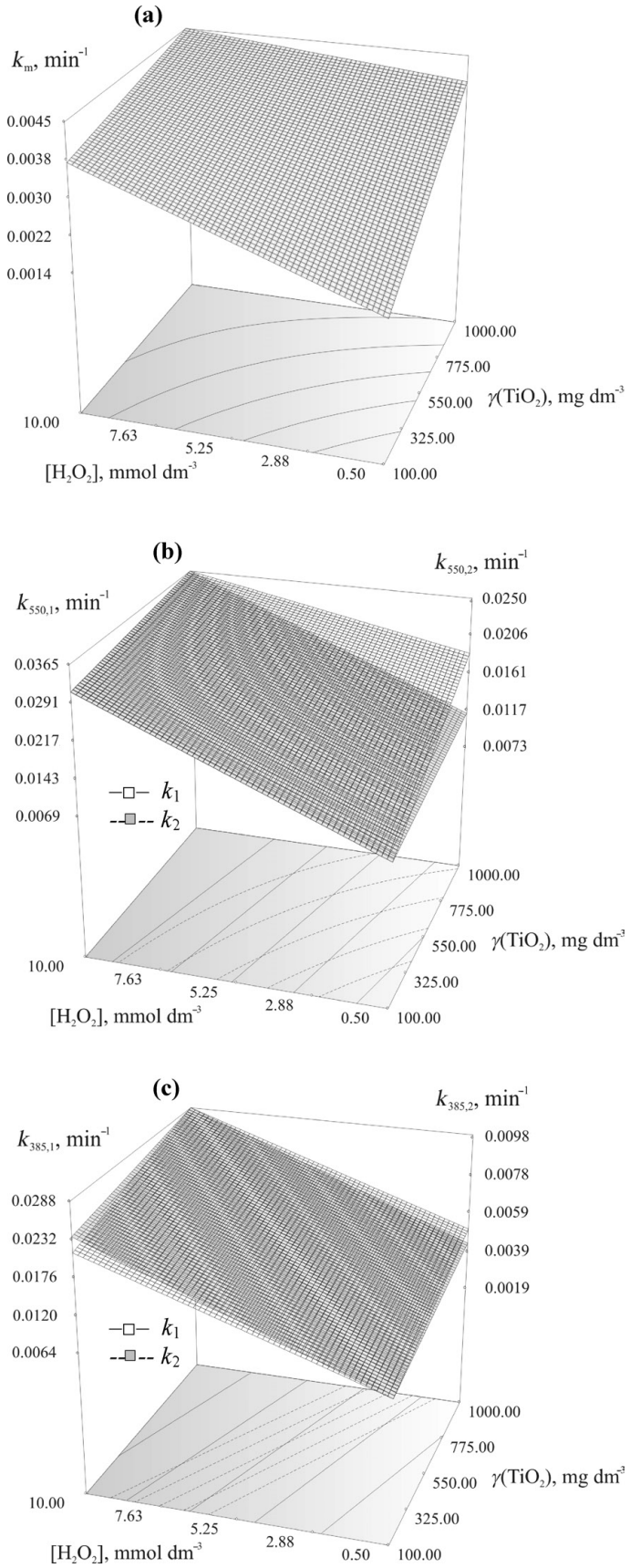

F i g . 6 (a – c) – *Graphic interpretation of the model that describes dependency of observed responses to process parameters and their interactions at fixed initial pH value of the system (pH 3); UV/TiO_2/H_2O_2 process*

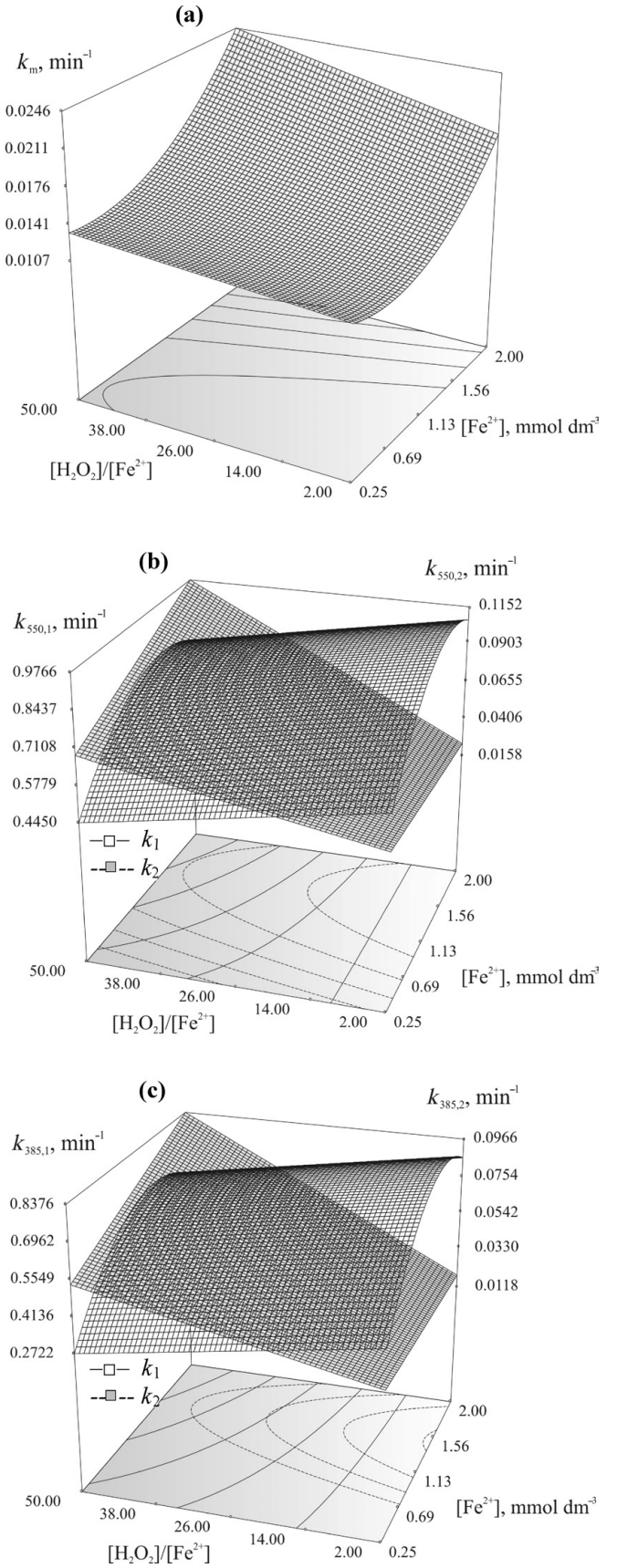

F i g . 7 (a – c) – *Graphic interpretation of the model that describes dependency of observed responses to process parameters and their interactions at fixed initial pH value of the system (pH 3); [Fe^{2+}]/[H_2O_2] process*

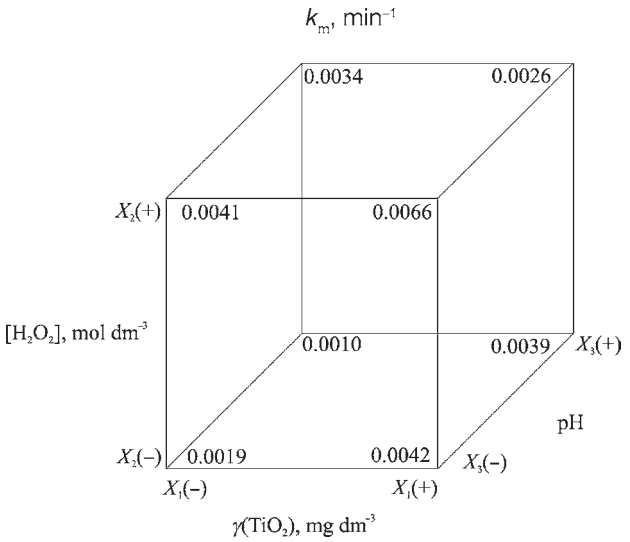

F i g . 8 – *Cube graph for different factors affecting applied UV/TiO_2/H_2O_2 process in terms of apparent mineralization rate constant*

ency of mineralization and decolourization rates on initial concentration of ferrous ions, X_{1F}, and initial Fenton ratio, X_{2F} at fixed pH (pH 3), is presented in Fig. 7a-c. The highest mineralization rate constant was achieved at high level of these CFs, according to Fig. 7a. Decolourization of model dye wastewater is not so well defined. In order to obtain expectable decolourization extent it is necessary to compromise between high and low level of CFs. In the first 5 min, decolourization at both wavelengths, λ = 550 and 385 nm, is fast and does not acquire a lot of Fenton reagent. On the other hand, the second step of decolourization is somewhat slower; $k_{2\,\lambda\,max}$ rapidly decreases with smaller initial amounts of both reagents (Fe^{2+} and H_2O_2). The possible explanation could be a consummation of hydrogen peroxide throughout the process,[15] meaning different 'initial' operating conditions for decolourization of a starting dye and its intermediates, respectively. As presented in Fig. 7b and c, the optimal range of ferrous ions concentration could be observed regarding $k_{1\,\lambda\,max}$; from 1 to 1.6 mmol dm^{-3} at different Fenton ratios. Also, presentation of results of Fenton process at fixed initial pH value (pH 3) is found to be representative.[10,15,19]

When comparing applied processes, photocatalytic oxidation, UV/TiO_2/H_2O_2 and classic Fenton oxidation, [Fe^{2+}]/[H_2O_2], in the term of mineralization and decolourization rate constants, it could be observed that the Fenton process is faster than the photocatalytic process. Pseudo-first order mineralization rate achieved during the Fenton process, k_{mF} = 0.0213 min^{-1}, is approximately three times higher than the one achieved during the photocatalysis at the optimal conditions, k_{mUV} = 0.0065 min^{-1}. Furthermore, decolourization in the studied system is almost instantaneous when applying the Fenton process. On the other hand, the photocatalytic process implies some advantages,[20–22] and it could be easily applied and maintained for different types of wastewater. However, in this particular case, it is rather difficult to evaluate comparatively these processes on a laboratory scale. With this in mind, it could be concluded that both the applied processes resulted with high mineralization and decolourization extents, and therefore, the results obtained within this work present a solid basis whereas treatment of wastewaters loaded with organic dyes are taken into consideration.

Conclusions

Mineralization of miscellaneous dye solutions, containing 50 mg dm^{-3} RV2 and 50 mg dm^{-3} RY3 was described by pseudo-first order kinetics with the highest observed rate coefficients k_{mUV} = 0.0065 min^{-1} in the case of UV/TiO_2/H_2O_2 and k_{mF} = 0.0213 min^{-1} for the [Fe^{2+}]/[H_2O_2] process respectively. At the same time, decolourization of the studied system was defined by the two first order in-series reaction models which include degradation of RV2 or RY3 to intermediates in the first step, and a consequent degradation of intermediates towards product with zero absortivities at λ_{max} in the second step. The highest observed decolourization rates are as follows; $k_{1,550\ UV}$ = 0.040 min^{-1}, $k_{2,550\ UV}$ = 0.017 min^{-1}, $k_{1,385\ UV}$ = 0.031 min^{-1}, $k_{2,385\ UV}$ = 0.010 min^{-1}, and $k_{1,550\ F}$ = 0.955 min^{-1}, $k_{2,550\ F}$ = 0.062 min^{-1}, $k_{1,385\ F}$ = 0.904 min^{-1}, $k_{2,385\ UV}$ = 0.099 min^{-1}.

The statistical study of UV/TiO_2/H_2O_2 and [Fe^{2+}]/[H_2O_2] process was performed using response surface method (RSM), i.e. D-optimal design. Initial TiO_2 mass concentration, initial hydrogen peroxide concentration, and initial pH were chosen as the determining factors for the performance of UV/TiO_2/H_2O_2 process, while initial [Fe^{2+}] concentration, oxidant/catalyst mole ratio, and initial pH were chosen as the key operating factors for the [Fe^{2+}]/[H_2O_2] process. F-values in the range from 6.59 to 30.67 and p-values < 0.0500 imply that each model equation obtained is significant concerning UV/TiO_2/H_2O_2. Predictive statistical models defining mineralization and decolourization rates achieved by the Fe^{2+}/H_2O_2 process involved some quadratic terms, X_1^2, X_3^2, resulting in enhanced significance. Namely, F-values are in the range of 126.15 to 5316.28 and corresponding p-values are below 0.0001. Since the high mineralization and decolourization extents were achieved with the processes applied in the present work, these results present a solid basis for the treatment of wastewater loaded with organic dyes.

ACKNOWLEDGEMENT

This work was supported by the Croatian Ministry of Science, Education and Sport, Project #125-1253092-1981.

List of symbols

b_n – coefficient associated with each n^{th} factor
c – molar concentration, mol dm^{-3}
h – chosen design points
h^+ – proton hole
K – adsorption coefficient of the reactant
k – rate constant, min^{-1}
r – reaction rate, mol dm^{-3} min^{-1}
n – candidate points
r^2 – correlation coefficient
t – time, min
V – volume, dm^3
w – mass fraction, %
X_1 – initial TiO_2 mass concentration
X_2 – initial H_2O_2 concentration
X_3 – initial pH
Y – response
[.] – molar concentration, mol dm^{-3}

Abbreviations

abs – absorbance
AOPs– advanced oxidation processes
CFs – control factors
DoE – Design of experiments
2FI – a two-factor-interaction model
L-H – Langmuir-Hinshelwood
$h\nu$ – photon of light
RSM – response surface method
RV2 – C.I. Reactive Violet 2
RY3 – C.I. Reactive Yellow 3
TOC – total organic carbon content, mg dm^{-3}

Greek letters

ε – molar extinction coefficient
λ – wavelength, nm
γ – mass concentration, g dm^{-3}
Θ – fraction of the surface covered by the reactant

Subscripts

app – apparent
F – Fenton process
i – refers to the studied process
m – mineralization
max – maximal
UV – photocatalytic oxidation
0 – initial

References

1. *Muruganandham, M., Swaminathan, M.,* Sep. Purif. Technol. **48** (2006) 297.
2. *Gupta, R. S.,* Environmental Engineering and Science, An Introduction, Government Institutes, Rockville, 1997.
3. *Malik, P. K., Sanyal, S. K.,* Sep. Purif. Technol. **36** (2004) 167.
4. *Ramirez, J. H., Costa, C. A., Madeira, L. M.,* Catal. Today **107–108** (2005) 68.
5. *Saravanathamizhan, R., Soloman, P. A., Balasubramanian, N., Ahmed Basha, C.,* Chem. Biochem. Eng. Q. **22** (2008) 213.
6. *Harir, M., Gaspar, A., Kanawati, B., Fekete, A., Frommberger, M., Martens, D., Kettrup, A., El Azzouzi, M., Schmitt-Kopplin, Ph.,* Appl. Catal. B: Environ. **84** (2008) 524.
7. *Chacón, J. M., Leal, M. T., Sánchez, M., Bandala, E. R.,* Dyes Pigments **69** (2006) 144.
8. *Grčić, I., Koprivanac, N., Vujević, D., Papić, S.,* J. Adv. Oxidation Technol. **11** (2008) 91.
9. *Grčić, I., Papić, S., Peternel, I., Koprivanac, N.,* 2nd International Congres on Green Process Engineering & 2nd European Process Intensification Conference (GPE-EPIC 2009), Proceedings.
10. *Koprivanac, N., Vujević, D.,* Int. J. Chem. Reactor Eng. **5** (2007) A56.
11. *Grčić, I., Mužic, M., Vujević, D. Koprivanac, N.,* Chem. Eng. J. **150** (2009) 476.
12. *Ray, S., Lalman, J. A., Biswas, N.,* Chem. Eng. J. **150** (2009) 15.
13. *Bergamini, R. B. M., Azevedo, E. B., Raddi de Araújo, L. R.*, Chem. Eng. J. **149** (2009) 215.
14. *Julson, A. J., Ollis, D. F.,* Appl. Catal. B: Environ. **65** (2006) 315.
15. *Grčić, I., Vujević, D. Koprivanac, N.,* Chem. Eng. J. **157** (2010) 35.
16. *Zainal, Z., Hui, L. K., Hussein, M. Z., Abdullah, A. H., Hamadneh, I. R.,* J. Hazard. Mater. **164** (2009) 138.
17. *Wang, C., Zhang, X., Liu, H., Li, X., Li, W., Xu, H.,* J. Hazard. Mater. **163** (2009) 1101.
18. *Molina, R., Martínez, F., Melero, J. A., Bremner, D. H., Chakinala, A. G.,* Appl. Catal. B: Environ. **66** (2006) 198.
19. *Muthukumari, B., Selvam, K., Muthuvel, I., Swaminathan, M.,* Chem. Eng. J. **153** (2009) 9.
20. *Akpan, U. G., Hameed, B. H.,* J. Hazard. Mater. **170** (2009) 520.
21. *Zayani, G., Bousselmi, L., Mhenni, F., Gharabi, A.,* Desalination **246** (2009) 344.
22. *Jain, R., Shrivastava, M.,* J. Hazard. Mater. **152** (2008) 216.